A Morphological Study of Melt-Spun Polypropylene Filaments by Atomic Force Microscopy

JONI HAUTOJÄRVI,[1] ANTTI LEIJALA[2,*]

[1] J. W. Suominen Oy, P.O. Box 25, FIN-29251 Nakkila, Finland

[2] Laboratory of Processing and Heat Treatment of Materials, Helsinki University of Technology, P.O. Box 6200, FIN-02015 TKK, Finland

Received 12 November 1998; accepted 22 March 1999

ABSTRACT: Surface morphology of melt-spun polypropylene (PP) filaments, spun from an additive-free PP powder and from a commercial-grade PP with different draw ratios, were examined with atomic force microscopy (AFM). The surface morphology of as-spun filaments was spherulitic. The gradual transformation of the surface structure from a spherulitic morphology to a fibrillar morphology during stretching was studied. In the filaments spun from the commercial-grade PP, the transformation was initiated by deformation of spherulites with a draw ratio of 1.2 and continued with association of lamellar stacks into fibrillar chains with a draw ratio between 1.2 and 2.0. A hierarchical morphological microstructure of fibrils, microfibrils, and nanofibrils was developed with a draw ratio of 4.0. In the filaments spun from the additive-free PP, the association of lamellar stacks into fibrillar morphology occurred considerably later, between draw ratios of 2.0 and 4.0. An oriented lamellar structure was found in these filaments, still with a draw ratio of 4.0. © 1999 John Wiley & Sons, Inc. J Appl Polym Sci 74: 1242–1249, 1999

Key words: polypropylene filament; melt-spinning; morphology; atomic force microscopy

INTRODUCTION

Polypropylene (PP) is the most widely used polyolefin polymer in the production of staple fibers and filaments for applications such as technical textiles, nonwovens, and high-tenacity yarns. The properties of PP fibers depend, to a great extent, on the morphology and surface microstructure of the fibers. Since spinning conditions, including spinning temperature, filament cooling, drawing, and thermal treatments, strongly affect the morphology of the fibers, the characterization of surface morphological features is of technological interest. So far, surface morphology of industrial PP fibers and filaments have not been studied extensively.

After the introduction of the first scanning force microscopy (SFM) technique, atomic force microscopy (AFM),[1] visualization of surface microstructures of insulating materials, even at the atomic scale, became available without sample pretreatment. Details about the SFM imaging techniques can be found in the literature.[2] Recently, these techniques have been widely applied for the characterization of morphological microstructures of various polymeric materials.[3,4] The spherulitic and lamellar morphology of syndiotactic PP[5–8] and isotactic PP[9–11] have been studied

* *Present address:* Nokia Telecommunications Inc., P.O. Box 300, FIN-00045 Nokia Group, Finland.

Correspondence to: J. Hautojärvi (E-mail: joni hautojarvi@jws.fi).

Journal of Applied Polymer Science, Vol. 74, 1242–1249 (1999)
 CCC 0021-8995/99/051242-08

extensively with SFM. The determination of molecular parameters, such as lamellar thickness,[9,11] a long period,[5] and chain-to-chain distance,[10] from AFM images have agreed well with the values determined by X-ray diffraction. However, tip-sample interactions during imaging small, sharp features cause some uncertainity as to the values measured by SFM images.

Investigations of oriented PP have revealed the fibrillar microstructure from microfibrils (1-μm diameter) to nanofibrils (10-nm diameter) formed by extended PP chains,[12] as well as shish-kebab structures.[13] Oriented lamellar structures (row nucleated lamellae) have been studied on the surface of a microporous isotactic PP film (commercial Celgard-type membrane), where the long period along the fibrils was determined from AFM images.[14] Biaxially oriented, industrial isotactic PP films were found to have a branch-like structure of fibrillar features.[15] Corona treatment of the films resulted in the formation of drop-like features on the surface. Imaging the deformation of surface morphology of a melt-extruded PP film[16] and a hard elastic PP (HEPP) film[17] as a function of draw ratio have been done with an *in situ* stretching device connected to a SFM apparatus.

Various types of fibers have been studied by SFM. Studies of Kevlar fibers,[18,19] carbon fibers, graphite fibers;[20,21] and glass fibers,[22] as well as natural fibers, such as wool,[23] cellulose,[24] and collagen,[25] have been reported. High-modulus, gel-spun ultra-high molecular weight (UHMW) polyethylene (PE) fibers have been examined in liquid cell under water.[26] This study visualized the hierarchical microstructure of PE fiber surface, where microfibrils (30–50-nm diameter) are formed from a plurality of nanofibrils (5–7-nm diameter) that are the elemental construction units of the fiber. Only a few publications related to the studies of surface morphology of PP fibers by SFM techniques exist. Our previous study describes the characterization of spin finish layers on PP fiber surfaces by means of SFM.[27] In this article, we report the results of AFM studies on the surface morphology and microstructure of finish-free PP filaments. PP filaments, produced by melt-spinning from an additive-free PP powder and from a commercial-grade PP in laboratory scale with different draw ratios, were characterized. Our aim is to understand the development and transformation of surface morphology during filament stretching in industrial melt-spinning conditions, rather than to illustrate the molecular-scale features of PP.

EXPERIMENTAL

Polypropylene filaments with a titer of 30 dtex (corresponding to a diameter of about 70 μm) were melt-spun in laboratory scale with a Haake HBI System 90 rheometer. The spinneret had 10 holes with a diameter of 0.20 mm. The spinning temperature was 250°C; and the extruded filaments were quenched with air, having a temperature of 25°C. After spinning, the filaments were stretched on-line with a pair of godets with draw ratios varying from 1.0 (as-spun) to 4.0. The temperature during stretching stage was either 25 or 90°C. The raw materials used in the spinning were additive-free isotactic PP powder (Borealis Polymers Inc., Porvoo, Finland), and Moplen Z30S grade PP granulates (Montell Polyolefins Inc., Wilmington, DE).

The degree of crystallinity of the filaments was measured with wide-angle X-ray scattering (WAXS). The diffractometer used was a Philips PW 1710 diffractometer connected to a PW 1730 generator. The degree of crystallinity was determined from the three highest diffraction maximums.

For AFM imaging, filament specimens with lengths of about 5 mm were cut from individual filaments and fixed to a sample holder without any surface pretreatment. The AFM measurements were carried out with a Rasterscope 4000® system (Danish Micro Engineering Inc.) with an optical video microscope. The scanner had a maximum scanning area of 45 $\times$45 μm^2, and it was calibrated by using the images of a calibration grid. All measurements were performed in air with silicone tips (radius of curvature 10 nm) connected to a parallel-beam-type cantilever having a length of 450 μm (Nanoprobe, Digital Instruments Inc.). The spring constant of the cantilevers was in the range of 0.2–0.3 *N*/m. A loading force of 10 n*N* was used during imaging. All of the images were plane-fitted to correct the roundness of the filament surfaces. The longitudinal direction of the fibers in the AFM images presented in this study is the vertical direction of the image.

RESULTS AND DISCUSSION

A large number of scans were captured from the studied filament surfaces. Figure 1(a) and (b)

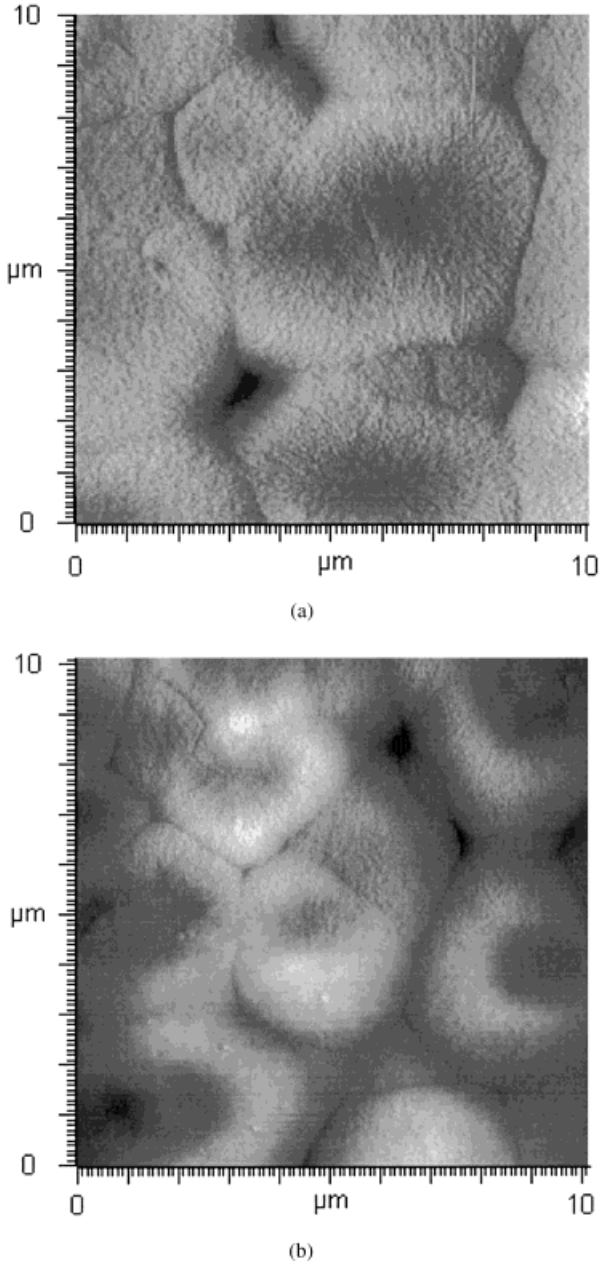

Figure 1 AFM images of as-spun PP filaments: (a) filament spun from the commercial-grade PPC (height difference, 270 nm) and (b) filament spun from the additive-free PP (height difference, 300 nm).

show typical 10 $\times$10 μm^2 AFM images of the 30 dtex PP filaments with draw ratios of 1.0 (as-spun) spun from the commercial PP grade [Fig. 1(a)] and from the additive-free PP grade [Fig. 1(b)]. The degree of crystallinity of the filaments was 30 and 35%, respectively, as determined from the WAXS measurements. The surface structure of the filaments show a spherulitic morphology with the diameter of spherulites varying between 1 and 10 μm. No differences could be detected in the overall morphologies between the samples spun from the two PP grades. Magnification of a spherulite in Figure 2(a) reveals a typical grain-like structure in the spherulites of the filaments spun from the commercial-grade PP. The grains, having a diameter in the 100–150-nm range, are slightly elongated in the direction of the fiber.

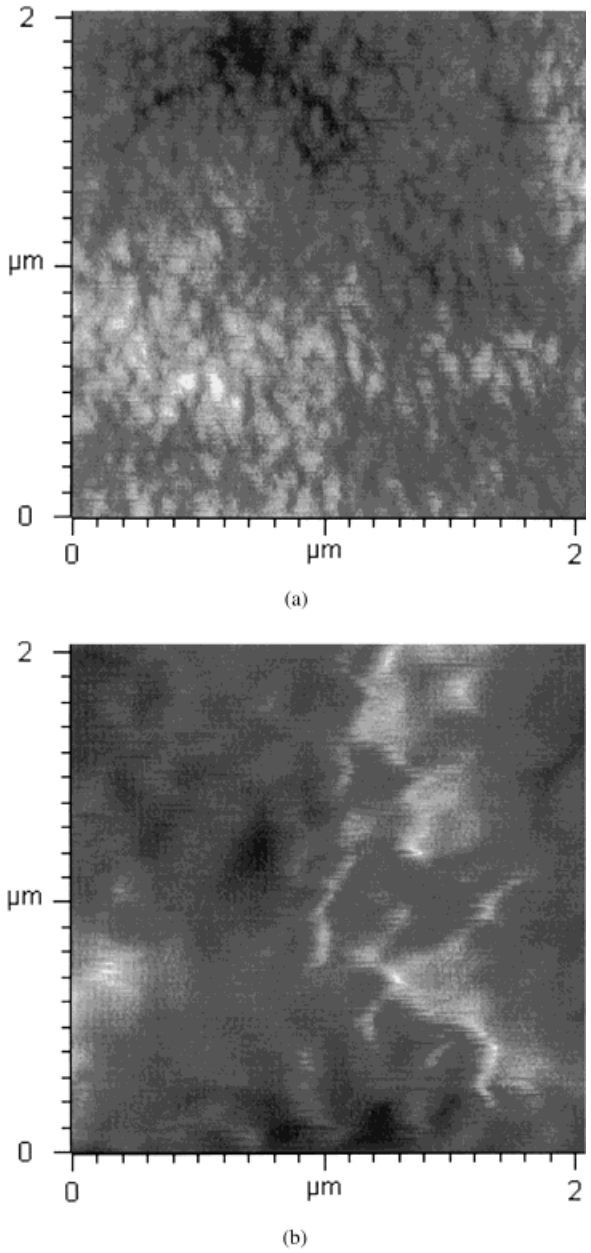

Figure 2 2 $\times$ 2 μm magnification of as-spun PP filaments: (a) commercial-grade PP (height difference, 34 nm) and (b) additive-free PP (height difference, 55 nm).

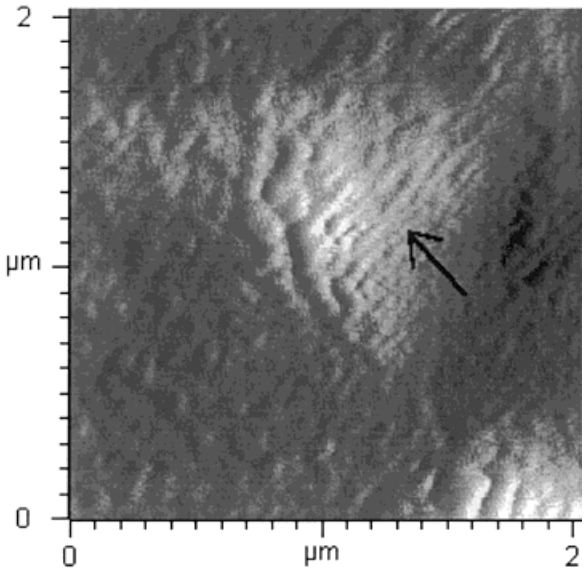

Figure 3 2 × 2 μm enlargement of the center of a spherulite in a filament spun from the additive-free PP with a draw ratio of 1.2. (Height difference, 66 nm.)

These grains consisted of ends of radial lamellar stacks protruding to a height of a few nanometers from the surface of the spherulite. This is consistent with the results of Crämer et al. reported in Magonov.[3] They have found from AFM measurements a width of 100–150 nm for radial lamellar blocks in spherulites of both syndiotactic PP and isotactic PP.

The surface of the spherulites in the filaments spun from the additive-free PP is smooth, and the grainlike structure could not be observed clearly in most of the images, as indicated by Figure 1(b). This is due to a soft layer of degraded PP that covers the surface of these filaments. The scanning tip deforms the soft layer of degraded PP with the imaging force used, as can be seen in the magnification in Figure 2(b). The existence of a layer of degraded PP is obvious since the additive-free PP does not contain antioxidants that prevent the degradation of the surface of the polymer during melt-spinning. When the draw ratio was increased to 1.2, filaments spun from the additive-free PP showed a spherulitic structure similar to Figure 1(a). Enlargement of the center of a spherulite is shown in Figure 3, where tangential lamellar stacks parallel to the surface were found, as indicated by the arrow. The lamellar stacks have a width of about 50 nm, and they consist of several edge-on lamellae. The angle between the direction of the filament and the tangential lamellar stacks is about 45°. On the left-hand side of the image, the grainlike structure of radial lamellar stacks is dominating. This observed crosshatched lamellar structure indicates that the spherulite is probably of α-type. Detailed examination of the spherulite types and the determination of the fraction of α- and β-spherulites could not be done for the reason that the filament specimens were not etched in order to remove the amorphous material.

The structure of the filaments spun from the commercial-grade PP with the draw ratio of 1.2 is shown in Figure 4(a). The overall surface morphology consists of fibrillar features oriented along the direction of stretching. The width of the fibrils is in the range of 0.5–1 μm. The smooth plateau in the upper right corner in the image is an artifact caused by an occasional loss of contact of the tip with the surface during imaging. Edges of the fibrils have curved shapes, and grooves can be observed between the individual fibrils. Magnification of a fibril in Figure 4(b) indicates that the fibrillar features are chains of deformed spherulites. Curvature of the spherulites is observed on the edges of the imaged fibril. Crosshatched radial and tangential lamellar stacks, having a width in the range of 60–100 nm, can be observed on the surfaces of the deformed spherulites. The two fibrillar chainlike features connecting the deformed spherulites in Figure 4(b) give rise to the formation of microfibrils. Upon stretching, the lamellae in the spherulites orientate in the direction of stretching and associate into chains that have a width of about 200–300 nm. These chains of lamellar stacks represent the initial stage of microfibrils, where lamellae crossing the fibrillar chains to the perpendicular direction can be observed as well.

After increasing the draw ratio to 2.0, the formation of microfibrils in the filaments spun from the commercial-grade PP was completed. This is demonstrated in Figure 5(a),where an image of the surface of a filament spun with the draw ratio of 2.0 is shown. The dominant morphological features of the surface are the numerous microfibrils with a width of about 100 nm. The microfibrils in the image are associated into larger fibrils having a width varying from 2 to 4 μm. The enlargement of a fibril in Figure 5(b) reveals that the individual microfibrils are formed by oriented lamellar stacks. The average orientation angle of the lamellar stacks is about 20° with respect to the direction of stretching. The length of an individual stack varies between 200 and 400 nm. Upon further stretching to a draw a ratio of 4.0, the

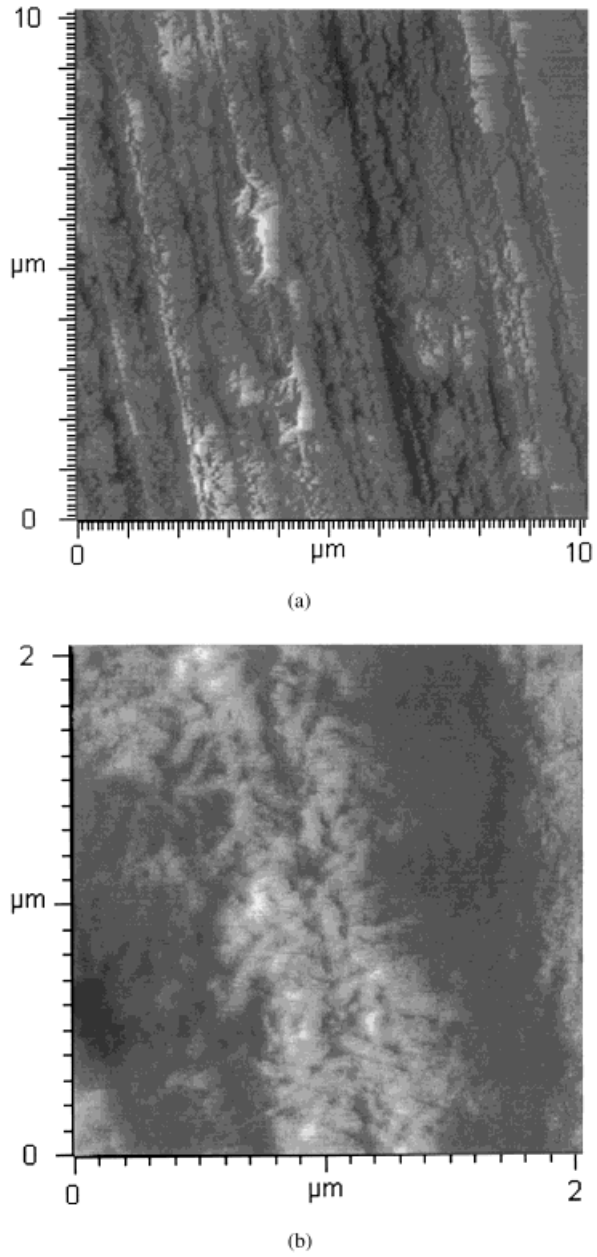

Figure 4 AFM images of a filament spun from the commercial-grade PP with a draw ratio of 1.2: (a) 10 × 10 μm image (height difference, 120 nm); (b) 2 × 2 μm image (height difference, 68 nm).

lamellar stacks orientate completely to the stretching direction and transform into individual nanofibrils, as illustrated in Figure 6(a) and (b). In Figure 6(a), the main surface features are the microfibrils with a width on the order of hundreds of nanometers. The microfibrils are combined into larger fibrils having a width on the order of micrometers. The surface of the microfibrils show a rough structure with threadlike patterns. The substructure of the microfibrils is demonstrated in Figure 6(b). A microfibril is constructed of a plurality of nanofibrils having a width of about 30–50 nm. Lamellar platelets connecting two neighboring nanofibrils can also be observed. The existence of lamellar plateletes indicates that the nanofibrils are not fully extended. Since the sam-

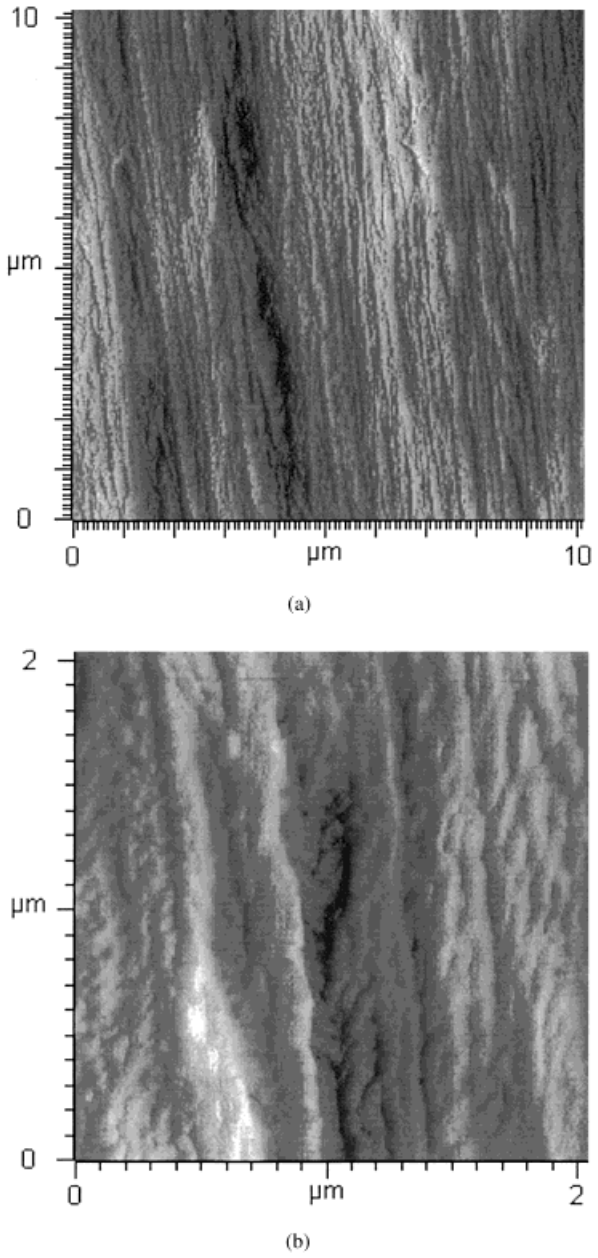

Figure 5 AFM images of a filament spun from the commercial-grade PP with a draw ratio of 2.0: (a) 10 × 10 μm image (height difference, 190 nm); (b) 2 × 2 μm image (height difference, 70 nm).

ples were imaged without a pretreatment, details about the morphology of an individual nanofibril could not be studied due to the amorphous material that covers the crystalline structures. Nanofibrils with a width in the 20–40 nm range of etched samples of drawn films of isotactic PP with a draw ratio of 6.0 have been studied previously.[13] The nanostructure of the fibrils in the film specimens were reported to consist of closely packed lamellar platelets with a repeat distance of 30–35 nm, representing the long period in a shish-kebab structure. The substructure of the nanofibrils that we have imaged is probably similar to those described in Crämer et al.,[13] although we did not get experimental proof for the morphology of the nanofibrils. However, it can be assumed that the basic construction units of the fibrils in these PP filaments with the draw ratio of 4.0 are shish-kebab nanofibrils. The nanofibrils probably have a stretched crystalline thread (shish), where lamellar platelets (kebab) are homoepitaxially grown. Further stretching would orientate the lamellar platelets, leading to the formation of smooth, extended-chain fibrillar morphology with the diameter of a nanofibril of about 10 nm.

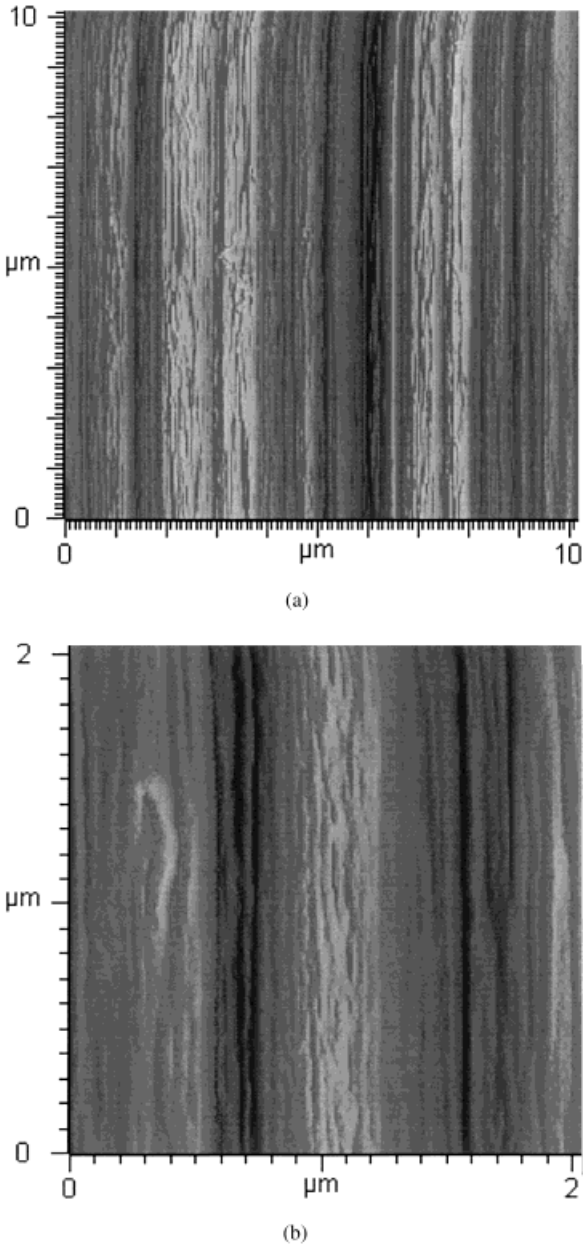

Figure 6 AFM images of a filament spun from the commercial-grade PP with a draw ratio of 4.0: (a) 10 × 10 μm image (height difference, 290 nm); (b) 2 × 2 μm image (height difference, 50 nm).

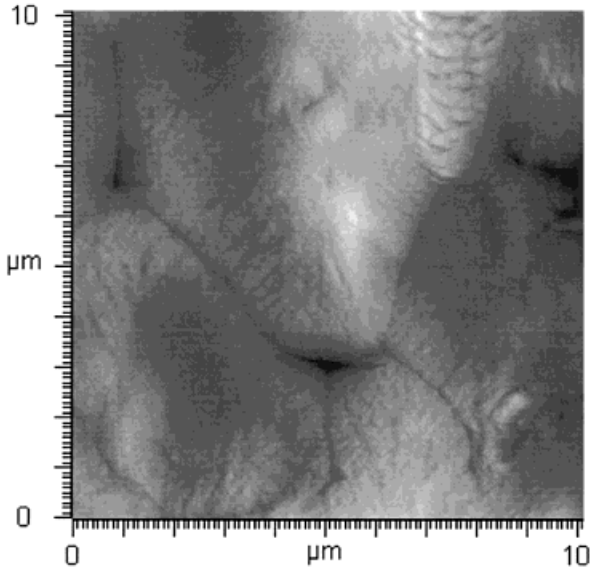

Figure 7 AFM image of a filament spun from the additive-free PP with a draw ratio of 2.0. (Height difference, 350 nm.)

The filaments spun from the additive-free PP had a spherulitic morphology with the draw ratio of 2.0. This is indicated in Figure 7, where an AFM image of the surface of a filament with the draw ratio of 2.0 is shown. The spherulites that are deformed in the direction of stretching, can be clearly observed. A rare morphologic feature, a cylindrite, having a width of 1.5 μm, can be seen in the upper right corner of the image. The dominating nanostructure of the spherulites are the ends of radial lamellar stacks that appear as a grainlike morphology with a grain width of 100–150 nm, similar to the structure shown in Figure 2(b). When the draw ratio was increased to the value of 4.0, transformation of the spherulitic

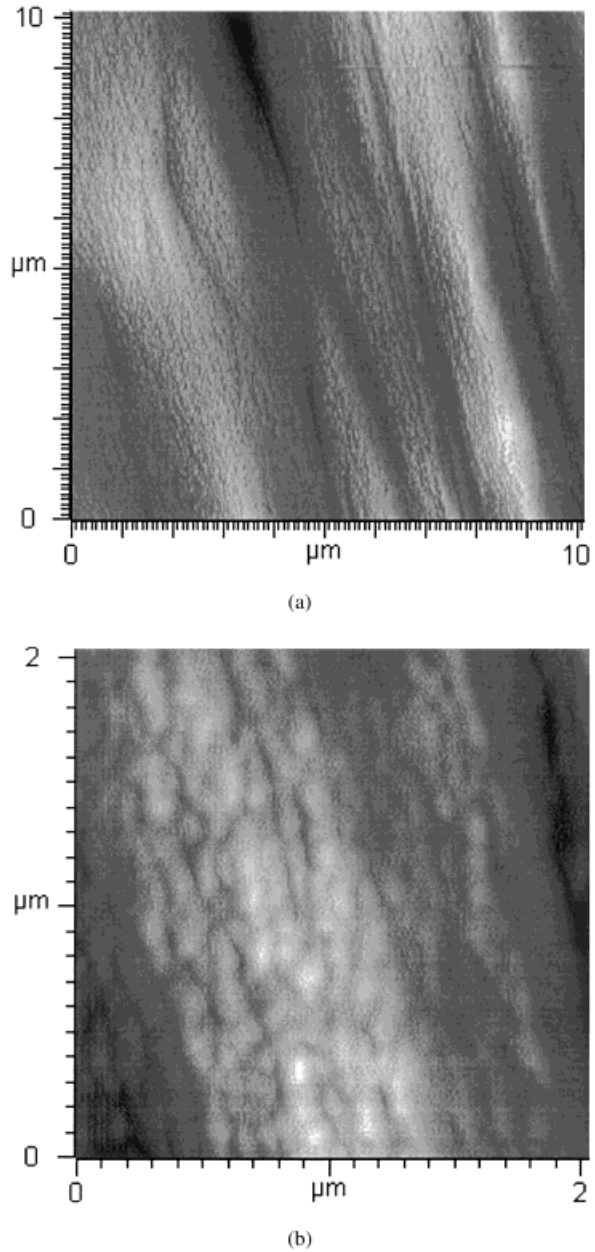

Figure 8 AFM images of a filament spun from the additive-free PP with a draw ratio of 4.0: (a) 10 × 10 μm image (height difference, 140 nm); (b) 2 × 2 μm image (height difference, 35 nm).

morphology to a fibrillar morphology was observed. Figure 8(a) shows the surface structure of a filament spun from the additive-free PP with a draw ratio of 4.0. The large fibrils with a width in the range of micrometers can be seen more clearly in Figure 8(a) than in the case of the commercial-grade PP in Figure 5(a). This is due to the layer of degraded PP that masks the microfibrillar structure. Enlargement of a fibril in Figure 8(b) shows an oriented lamellar morphology resembling the structure of a microfibril in Figure 4(b). Detailed examination of the substructure is limited due to the surface degradation. However, it can be assumed, based on the results obtained from the filaments spun from the commercial-grade PP, that the oriented lamellar stacks are associated into microfibrils that are further combined into the larger fibrils. The transformation of the morphology to the fibrillar structure is not completed yet at this stage. The development of the hierarchical morphological structure of fibrils, microfibrils, and nanofibrils occurs, probably in this case, with higher draw ratios than 4.0. The difference between the transformations of surface morphologies of filaments spun from the additive-free and commercial grades of PP can be explained by the nucleating effect of the additives. The additives with a small particle size increase the interfacial area in the polymer bulk in commercial PP grade, thus facilitating the fibrillation process. This leads to the transformation of surface morphology with lower draw ratios.

The effect of temperature on the structure of the filaments during stretching was studied. When the temperature of the stretching stage was 25 °C, the degree of crystallinity of the filaments, as determined by WAXS, was in the range of 20–35%, depending on the draw ratio used. After increasing the temperature of the stretching stage to 90°C, the crystallinity of the filaments increased to the range of 55–65%. However, when comparing the AFM images obtained from the filaments stretched in different temperatures, no differences in the surface morphologies could be observed. This indicates that the crystallinity of the surface that crystallizes under the highest undercooling after spinning is high. Further crystallization during stretching in elevated temperature proceeds in the less-crystalline core of the filaments. Investigations of cross sections of the filaments by AFM would probably reveal a decreasing nucleation density from the surface down to the core.

CONCLUSIONS

AFM studies of PP filaments demonstrated the gradual transformation of the surface morphology from a spherulitic morphology to a fibrillar morphology during stretching. The surface structure of as-spun filaments was spherulitic. The trans-

formation of the spherulitic morphology into the fibrillar morphology was initiated by deformation of the spherulites and orientation of lamellar stacks into microfibrillar chains. The transformation was completed by association of lamellar stacks into nanofibrils. At this stage, the filaments showed a hierarchical fibrillar structure, including fibrils (width in the order of micrometers), microfibrils (width in the order of hundreds of nanometers), and nanofibrils (width in the order of tens of nanometers). Filaments spun from the commercial-grade PP transformed into a fibrillar morphology between draw ratios of 1.2 and 2.0. The corresponding draw ratio with the filaments spun from the additive-free PP was between 2.0 and 4.0. The increase of crystallinity during stretching in an elevated temperature did not change the surface morphology, as observed by AFM.

The authors thank R&D Director, Dr. Margareta Huldén, from J. W. Suominen Oy and Professor Antti Korhonen from Helsinki University of Technology, Laboratory of Processing and Heat Treatment of Materials, for their support during this work.

REFERENCES

1. Binnig, G.; Rohrer, H.; Gerber, C.; Weibel, E. Phys Rev Lett 1986, 56, 930.
2. Magonov, S.; Whangbo, M.-H. Surface Analysis with STM and SPM; VCH: Wenheim, Germany, 1996.
3. Magonov, S. N. Polym Sci, Ser B. 1996**,** 38, 34.
4. Tsukruk, V. V. Rubber Chem Technol 1997*,*70, 430.
5. Thomann, R.; Wang, C.; Kressler, J.; Jüngling, S.; Mülhaupt, R. Polymer 1995, 36, 3795
6. Stoker, W.; Magonov, S. N.; Cantonow, H.-J.; Wittmann, J. C.; Lotz, B. Macromolecules 1993, 26, 5915.
7. Stocker, W.,: Schumacher, M.; Graff, S.; Lang, J.; Wittmann, J. C.; Lovinger, A. J.; Lotz, B. Macromolecules 1994, 27, 6948.
8. Tsukruk, V. V.; Reneker, D. H. Macromolecules 1995*,* 28, 1370.
9. Schönherr, H.; Snétivy, D.; Vancso, J. Polym Bull 1993, 30, 567.
10. Snévity, D.; Guillet, J. E.; Vancso, G. J. Polymer 1993, 34, 429.
11. Vancso, G. J.; Nisman, R.; Snétivy, D.; Schönherr, H.; Smith, P.; Ng, C.; Yang, H. Colloids Surf. A: Physicochem. Eng. Asp 1994, 87, 263.
12. Snévity, D.; Vancso, G. J. Polymer 1994, 35, 461
13. Crämer, K.; Schneider, M.; Mülhaupt, R.; Cantow, H.-J.; Magonov, S. N. Polym Bull 1994*,* 32, 637.
14. Chen, R. T.; Saw, C. K.; Jamieson, M. G.; Aversa, T. R.; Callahan, R. A. J Appl Polym Sci 1994, 53, 471.
15. Vancso, G. J.; Allston, T. D.;Chun, I.; Johansson, L.-S.; Liu, G.; Smith, P. F. Int J Polym Anal Charact 1996, 3, 89.
16. Hild, S.; Marti, O. Polym Prepr (Am Chem Soc, Div Polym Chem) 1996; 37, 569.
17. Hild, S.; Gutmannsbauer, W.; Lüthi, R.; Fuhrmann, J.; Güntherodt, H.-J. J Polym Sci, Part B: Polym Phys 1996, 34, 1953.
18. Glomm, B. H.; Grob, M. C.; Neuenschwander, P.; Suter, U. W.; Snétivy, D.; Vancso, G. J. Polym Commun 1994, 35, 878.
19. Rebouillat, S.; Donnet, J.-B.; Wang, T. K. Polymer 1997, 38, 2245.
20. Dzenis, Y.; Reneker, D. H.; Tsukruk, V. V.; Patil, R. Comp Interfaces 1994, 2, 307.
21. Endo, M.; Oshida, K.; Kobori, K.; Takeuchi, K.; Takahashi, K. J Mater Res 1995, 10, 1461.
22. El Achari, E.; Ghenaim, A.; Wolff, V.; Caze, C.; Carlier, E. Textile Res J 1996, 66, 483.
23. Phillips, T. L.; Horr, T. J.; Huson, M. G.; Turner, P. S.; Shanks, R. A. Textile Res J 1995, 65, 445.
24. Hanley, S. J.; Giasson, J.; Revol, J.-F.; Gray, D. G. Polymer 1992, 33, 4639.
25. Chernoff, E. A. G.; Chernoff, D. A. J Vac Sci Technol, A, 1992, 10, 596.
26. Wawkuschewski, A.; Cantow, H.-J.; Magonov, S. N.; Hewes, J. D.; Kocur, M. A. Acta Polym 1995, 46, 168.
27. Leijala, A.; Hautojärvi, J. Textile Res J 1998, 68, 193.